

### Stabilisation of Double Excited Induction Machine Used in WECS in Two Modes of Operation

العمل على استقرار الآلة الحثية ذات التغذية المزدوجة المستخدمة في نظم  
تحويل طاقة الرياح إلى طاقة كهربائية لحالتين من حالات التشغيل .

M. T. El-Hagry                      A. A. Mohamed                      N. N. Iskander  
Elect. Research Inst.                  Faculty of Engg.                  Elect. Research  
NRC                                      Menoufia Univ.                      Inst. NRC

خلاصة : يقدم هذا البحث طريقة جديدة للعمل على استقرار الآلة الحثية ذات التغذية  
المزدوجة لحالتين من حالات التشغيل حيث أنه في الحالة الأولى يستخدم القوم  
العاكس للجهد بينما في الحالة الثانية يستخدم القوم العاكس للتيار . وتمتد  
هذه الطريقة على التحكم في الجهد المغذي للعضو الدوار مقداراً واتجاهاً حتى  
يحظى اداً مستقر عند السرعات المختلفة . وقد تم دراسة تأثير بعض المتغيرات  
الهامة بفرض زيادة مدى استقرار الآلة .

#### ABSTRACT

The stability of the DEIM used in WECS in two modes of operation is completely investigated. In the first mode a voltage fed inverter is proposed in the rotor circuit, while a current fed inverter is proposed in the second mode. To maintain the DEIM stable from  $S=-1$  to 1. A control strategy is proposed by varying the magnitude and phase angle of the applied rotor voltage. Also the effect of some machine parameters on the DEIM stability is investigated.

#### INTRODUCTION

The double excited induction machine (DEIM) is an induction machine fed from the stator with voltage at power frequency, and from the rotor with voltage at slip frequency. It is characterised by higher torque capability at smaller frame size and within wide range of operating speeds. It was proved in a previous research [1] that by adjusting the rotor voltage magnitude and phase angle, the DEIM could operate as a generator at subsynchronous speeds. These characteristics renders the DEIM attractive for use in wind energy conversion schemes (WECS). However, the drawback of such machine is its inherent instability due to the presence of negative damping torque. Previous work [2] showed that using a constant-current source inverter in the rotor circuit renders the DEIM stable within slip range from  $S=-1$  to  $S=+1$ . However the time response showed that on the application of a step load torque, the oscillation decayed slowly since only the mechanical damping of the motor acts on the system. They proposed a current controller to assure stable operation and accelerate the decay of oscillation.

Stabilising the DEIM with voltage source inverter in the rotor circuit was tried before [3,4] by changing the machine parameters, however this method was not effective for wide speed ranges. Stabilising the DEIM using a linear speed feedback system was suggested by Ohi [5] which is doubtful since the negative damping torque is not a linear function of speed.

In this paper the dynamic behaviour of the DEIM in two modes of operation, with voltage source inverter (VSI) and then with current source inverter CSI, is completely investigated. In the first mode, the rotor circuit is connected to a line commutated voltage source inverter which supply the rotor with voltage at slip frequency. The inverter could be operated also as a rectifier if slip energy recovery scheme is to be applied.

In the second mode of operation, the rotor circuit is connected to a constant current inverter whose current is fixed to the rated current of the induction machine. Another value of rotor current is assumed and the stability results are compared.

A novel method for stabilising the DEIM with a voltage source inverter without changing the machine parameters is also proposed.

**DYNAMIC BEHAVIOUR OF DEIM**

**1. DEIM with voltage source inverter:**

**a- Non-linear model**

For the synchronously rotating reference frame, d-q, the terminal relations of the machine are given by:

$$\begin{bmatrix} V_{ds} \\ V_{qs} \\ V_{dr} \\ V_{qr} \end{bmatrix} = \begin{bmatrix} R_s + L_s P & -\omega_s L_s & M_o P & -\omega_s M_o \\ \omega_s L_s & R_s + L_s P & \omega_s M_o & M_o P \\ M_o P & -S\omega_s M_o & R_r + L_r P & S\omega_s L_r \\ S\omega_s M_o & M_o P & S\omega_s L_r & R_r + L_r P \end{bmatrix} \begin{bmatrix} I_{ds} \\ I_{qs} \\ I_{dr} \\ I_{qr} \end{bmatrix} \quad (1)$$

The equation of motion for the machine is

$$T_e = \frac{J}{np} \frac{d\omega_m}{dt} + \frac{K_d}{np} \omega_m + T_L \quad (2)$$

and

$$T_e = 1.5 np M_o (I_{qs} I_{dr} - I_{ds} I_{qr})$$

The nonlinear equations (1-3) are solved numerically using Rung-Kutta [4] method. The results revealed the unstable operation of the DEIM on applying a step load torque at S=0.3. The rotor speed deviations versus time when applying a torque to the machine is shown in Fig. (1).

**b- Linearized dynamic model and transfer function:**

In order to derive a method to stabilize the DEIM with VSI, the non-linear state Eqs.(1-3) are linearized by applying the small signal Taylor expansion around a steady state operating point represented by a subscript o.

The linearized equation become:

$$\Delta V_{ds} = (R_s + L_s P) \Delta I_{ds} - X_s \Delta I_{qs} + M_o P \Delta I_{dr} - X_m \Delta I_{qr} \quad (4)$$

$$\Delta V_{qs} = X_s \Delta I_{ds} + (R_s + L_s P) \Delta I_{qs} + X_m \Delta I_{dr} + M_o P \Delta I_{qr} \quad (5)$$

$$\begin{aligned} \Delta V_{dr} = & M_o P \Delta I_{ds} - M_o(\omega_s - \omega_{mo}) \Delta I_{qs} + (R_r + L_r P) \Delta I_{dr} \\ & - L_r(\omega_s - \omega_{mo}) \Delta I_{qr} + (M_o I_{qso} + L_r I_{qro}) \Delta \omega_m \end{aligned} \quad (6)$$

$$\begin{aligned} \Delta V_{qr} = & M_o(\omega_s - \omega_{mo}) \Delta I_{ds} + M_o P \Delta I_{qs} + L_r(\omega_s - \omega_{mo}) \Delta I_{dr} \\ & + (R_r + L_r P) \Delta I_{qr} - (M_o I_{dso} + L_r I_{dro}) \Delta \omega_m \end{aligned} \quad (7)$$

$$T_e = 1.5 np M_o (I_{qso} \Delta I_{dr} + I_{dro} \Delta I_{qs} - I_{dso} \Delta I_{qr} - I_{qro} \Delta I_{ds}) \quad (8)$$

$$\Delta T_L = T_e - \left( \frac{JP}{np} + \frac{K_d}{np} \right) \Delta \omega_m \quad (9)$$

For the synchronously rotating reference frame the voltage components are given by:

$$\begin{bmatrix} V_{ds} \\ V_{qs} \\ V_{dr} \\ V_{qr} \end{bmatrix} = \begin{bmatrix} V_{sm} \\ 0 \\ V_{rm} \cos(\theta_m + \phi) \\ -V_{rm} \sin(\theta_m + \phi) \end{bmatrix} \quad (10)$$

where :  $\theta_m$  is the torque angle.

$\phi$  is the phase angle between the applied rotor voltage and the stator reference voltage.

Perturbation about the operating point result in the following expressions:

$$\begin{bmatrix} \Delta V_{ds} \\ \Delta V_{qs} \\ \Delta V_{dr} \\ \Delta V_{qr} \end{bmatrix} = \begin{bmatrix} \Delta V_{sm} \\ 0 \\ -V_{rmo} \sin(\theta_{mo} + \phi) \Delta \theta_m + \Delta V_{rm} \cos(\theta_{mo} + \phi) \\ -V_{rmo} \cos(\theta_{mo} + \phi) \Delta \theta_m - \Delta V_{rm} \sin(\theta_{mo} + \phi) \end{bmatrix} \quad (11)$$

$$\omega_m = p\theta_m$$

Substituting Eq.(11) into Eqs.(4-9) and after manipulation, the transfer function,  $\Delta \omega_m / \Delta T_L$ , of the DEIM is obtained. it was found that the order of characteristic equation of this system is of the 10<sup>th</sup> degree. Neglecting the stator resistance, which is practical for large machines where  $R_s \ll L_s$ , the order of transfer function and the characteristic equation will be reduced greatly, then

The transfer function is :

$$\frac{\Delta \omega_m}{\Delta T_L} = \frac{np(C_1 p^3 + C_2 p^2 + C_3 p)}{H_4 p^4 + H_3 p^3 + H_2 p^2 + H_1 p + H_0} \quad (12)$$

where,

$$C_1 = (M_o^2 - L_r L_s)^2 / L_s^2$$

$$C_2 = -2R_s C_1$$

$$C_3 = R_r^2 + S^2 C_1$$

$$H_4 = C_1 J$$

$$H_3 = C_2 J + C_1 K_d$$

$$H_2 = C_3 J + C_2 K_d - np^2 M_o (C_4 E_1 - C_5 D_1)$$

$$H_1 = C_3 K_d' - np^2 M_o (C_4 E_2 - C_5 D_2)$$

$$H_o = np^2 M_o (C_5 D_3 - C_4 E_3)$$

$$C_4 = I_{qso} + M_o I_{qro} / L_s$$

$$C_5 = I_{dso} + M_o I_{dro} / L_s$$

$$D_1 = -A_3 A_4$$

$$D_2 = B_2 A_3 + R_r A_4 - SA_2 A_3$$

$$D_3 = -SA_3 B_1 - B_2 R_r$$

$$E_1 = A_2 A_3$$

$$E_2 = B_1 A_3 - A_2 R_r - SA_3 A_4$$

$$E_3 = SA_3 B_2 - B_1 R_r$$

The characteristic equation is given by :

$$H_4 P^4 + H_3 P^3 + H_2 P^2 + H_1 P + H_o = 0 \quad (13)$$

The solution of Eq.(13) is obtained using Newton-Raphson method. The roots of the characteristic equation are calculated for the slip range  $-1 \leq S \leq +1$ .

The DEIM is known to be unstable within most of its operating range due to the presence of negative damping torques. To maintain the DEIM stable within the whole range of slips considered, a control strategy is proposed by varying the magnitude  $V_r$  and phase angle " $\theta$ " of the applied rotor voltage. The effect of varying  $V_r$  and " $\theta$ " on the stability of the DEIM at positive slip is shown in tables I to III, where the stable points of operation are shown as small circles.



**Table III**

$$|V_r| = 0.2 |V_s|$$

$\theta^\circ \backslash S$	0.1	0.2	0.3	0.4	0.5	0.6	0.7	0.8	0.9
0									
10									
20									
30									
40								o	o
50							o	o	o
60						o	o	o	o
70					o	o	o	o	o
80				o	o	o	o	o	o
90			o	o	o	o	o		
100			o	o	o	o			
110		o	o	o	o				
120	o	o	o	o					
130	o	o	o						
140	o	o							
150	o	o							
160	o								
170	o								
180									

Tables I-III show the effect of rotor voltage magnitude and phase angle on the stable operating points of DEIM.

From Tables I-III, it is deduced that the DEIM with VSI in the rotor circuit could be stabilized at each slip by applying a voltage of certain magnitude and phase angle which differs at different values of slip. It is also noted that as  $V_r$  increases the range of angles within which the DEIM operates stably becomes wider except at  $S=0.1$ . It is also noted that as the speed decreases the range of stable operation is shifted by about  $10^\circ$  while the range itself is constant. Thus it can be concluded that with suitable choice of  $V_r$  and  $\theta$ , stable operation can be obtained.

For stable operation, the variation of active power generated or consumed as a percentage of rated machine power " $P_a$ ", with the phase angle  $\theta$  for different magnitudes of applied rotor voltages at subsynchronous speeds is shown in Figs. 1 to 3. From Fig. (2.a) it is noted that at  $V_r = .05 V_s$  the machine operates as a motor at all slips. In Fig. (2.b) at  $V_r = 0.1 V_s$ , and  $S > 0.15$  the machine operates as a stable double excited induction motor, while for lower slips it operates as a stable double excited induction generator.

In Fig. (3), at  $V_r = 0.2 V_s$ , and  $S > 0.2$  the machine operates as a stable double excited induction motor while for  $S \leq 0.2$  it operates as a stable double excited induction generator as has been shown before [1] which is reflecting on increasing the efficiency of converting wind energy



**Table VI**  
 $|V_r| = 0.2 \quad |V_s|$

$\theta^\circ \backslash s$	-0.1	-0.2	-0.3	-0.4	-0.5	-0.6	-0.7	-0.8	-0.9	-1.0
180	o									
190	o									
200	o	o								
210	o	o								
220		o	o							
230		o	o	o	o					
240		o	o	o	o	o	o			
250			o	o	o	o	o	o	o	o
260				o	o	o	o	o	o	o
270				o	o	o	o	o	o	o
280					o	o	o	o	o	o
290							o	o	o	o
300								o	o	o
310									o	o
320										o
330										
340										
350										

Tables IV to VI show the effect of rotor voltage magnitude and phase angle on stable operating points of DEIM for negative slips.

It is noted from tables IV to VI that increasing  $V_r$  has a negligible effect on the stability range at super-synchronous speeds. Also it can be noted that for speeds less than 1.5 synchronous speed, the stable range of  $\theta$  for each slip is different, while at higher speeds this range is slightly affected.

For stable operation at supersynchronous speeds, the variation of  $P_a$  with  $\theta$  for different magnitudes of  $V_r$  is shown in Figs. (4-6). It can be noted that:

- a) As  $\theta$  increases the consumed power increases reaching a maximum value and then falls.
- b) As  $V_r$  increases the power consumed increases i.e. the machine operation is going towards motoring, i.e. it is not possible to obtain stable generation with  $V_r > 0.1$ .

**EFFECT OF DEIM PARAMETERS**

The effect of increasing the rotor resistance on  $P_a$  at sub-and super-synchronous speeds is deduced from Fig. (7). It can be noted that as the rotor resistance  $R_r$  increases,  $P_a$  moves towards generating mode, i.e. stable generation mode can be obtained for  $R_r >$  twice the original value.

Fig. (8) gives the variation of the maximum power generated at different values of rotor resistance, with the slip. It is noted that as  $R_r$  increases the DEIM operates as a generator stably at higher speeds. However the maximum



power generated at a particular slip decreases as  $R_r$  increases. Fig.(9). shows the phase angle  $\phi$  at which maximum power is generated at each slip. From Figs.(8) and (9) the value of  $R_r$  and  $\phi$  for maximum power generation at each slip is deduced.

The effect of increasing the rotor reactance  $X_r$  on the active power consumed or generated by the DEIM at its stable operating points is shown in Fig.(10). By comparing this condition with the case at normal machine parameters, it is deduced that the active power consumed decreases as  $X_r$  increases. For instance, it is noted that at  $S = -1$  as  $X_r$  increases to 1.25 of its normal value the consumed power decreases to one half of its value at normal machine parameters. It is also noted that the DEIM still operates as a motor at supersynchronous speeds and that the stability range was not affected by increasing  $X_r$ . Thus it is deduced that if the DEIM has to be operated as a variable speed drive, increasing its rotor reactance decreases the active power consumption.

## 2. The DEIM with Current Source Inverter (CSI):

A current source inverter CSI, a d.c. link, and a rectifier are connected to the rotor circuit of the DEIM. The firing angle of inverter, is varied with speed variation to achieve constant rotor current. To study the stability of this scheme, the terminal machine equations (1-3) are solved first in the steady state for two values of constant rotor current, namely 0.75 and 1.0 of rated current. The steady state solution at different rotor current phase angles is obtained giving the initial operating points.

The non-linear Eqs.(1-3) are then linearized by applying the small signal Taylor expansion around the steady state operating points. The linearized equations become:

$$\Delta V_{ds} = (R_s + L_s P) \Delta I_{ds} - X_s \Delta I_{qs} + M_o P \Delta I_{dr} - X_m \Delta I_{qr} \quad (14)$$

$$\Delta V_{qs} = X_s \Delta I_{ds} + (R_s + L_s P) \Delta I_{qs} + X_m \Delta I_{dr} + M_o P \Delta I_{qr} \quad (15)$$

But since the machine is connected to the infinite bus bar, thus

$$\Delta V_{ds} = \Delta V_{qs} = 0$$

the constant current inverter configuration

$$I_{dr} = I_r \cos \delta \quad (16a)$$

$$I_{qr} = I_r \sin \delta \quad (16b)$$

$$\Delta I_{dr} = -I_{rm} \sin \delta_o \Delta \delta \quad (17a)$$

$$\Delta I_{qr} = I_r \cos \delta_o \Delta \delta \quad (17b)$$

The electrical torque equation is thus :

$$\Delta T_e = 1.5 n_p M_o I_r [(I_{dso} \cos \delta_o - I_{qso} \sin \delta_o) \Delta \delta + \sin \delta_o \Delta I_{ds} + \cos \delta_o \Delta I_{qs}] \quad (18)$$

The mechanical torque is given by :

$$\Delta T_L = \Delta T_e - (J P^2 + K_d P) \frac{\Delta \delta}{np} \quad (19)$$

Rearranging Eqs.(14 to 19) and after manipulation, the transfer function  $\Delta \omega_m / \Delta T_L$  of the DEIM with CSI is derived as follows:

$$\Delta \omega_m / \Delta T_L = np(A_3 P^3 + A_2 P^2 + A_1 P) / c.c. \quad (20)$$

where the characteristic Eq. c.c. is :

$$\begin{aligned} c.c. = & (A_3 J) P^4 + (A_2 J + A_3 K_d) P^3 - (I_r np^2 M_o E_3 - A_2 K_d - JA) P^2 \\ & - (I_r np^2 M_o E_2 - A_1 K_d) P - (I_r np^2 M_o E_1) \end{aligned} \quad (21)$$

where,

$$\begin{aligned} A_1 &= R_s^2 + X_s^2 \\ A_2 &= 2R_s L_s \\ A_3 &= L_s^2 \\ C &= I_{dso} \cos \delta_o - I_{qso} \sin \delta_o \\ E_1 &= CA_1 + I_r X_m X_s \\ E_2 &= CA_2 + I_r R_s M_o \\ E_3 &= CA_3 + I_r L_s M_o \end{aligned}$$

Solving the c.c. Eq.(21) shows that the DEIM with CSI is stable within the slip range  $-1 \leq S \leq 1$  at rotor current phase angle  $\delta$  ranging from  $180^\circ$  to  $359^\circ$ . To deduce the difference between the stable operating points at sub synchronous speeds, the power consumed or generated as a ratio of the rated machine power " $P_a$ " is plotted as a function of  $\delta$  in Fig. (11). It is noted that the DEIM with CSI operates as a generator at subsynchronous speed for phase angles ranging from  $280^\circ$  to  $355^\circ$  and  $S \leq 0.7$ , which is wider than in the case of DEIM with VSI and, as the speed decreases the generated power also decreases.

Fig.(12) shows  $P_a$  with  $S$  at super synchronous speeds. It is noted that power is generated at  $\delta > 270^\circ$  and as the speed increases the generated power increases and may reach 1.4 of the machine rated power at  $S = -1$ .

## CONCLUSIONS

This paper presents a novel method for stabilizing the OEIM in two modes of operation; and it was found that by properly controlling, the magnitude and phase angle of the applied rotor voltage, a stable operation can be obtained for slip variation between  $-1, 1$ .

Also the variation of active power generated or consumed with the phase angle for different magnitudes of applied rotor voltage was investigated. It has been shown that the increase of rotor voltage  $V_r$  increases the stability range, but it also increases the power consumption. So a proper choice of  $V_r$  and  $\theta$  to give lower power consumption and stable operation can be obtained readily from the tables given in this paper.

The effect of some important parameters on the DEIM showed that:

- 1- The DEIM could be operated stably, as generator, at super-and even at sub-synchronous speeds by varying  $R_r$ .
- 2- Increasing  $X_r$  decreases the input power needed to operate the DEIM stably with negative slip.

#### List of Symbols

R	resistance
X	self reactance
L	inductance
$M_o$	mutual inductance
$P_a$	ratio of active power to rated power in p.u. $= \frac{(V_{ds} I_{ds} + V_{dr} I_{dr} + V_{qs} I_{qs} + V_{qr} I_{qr})}{P_{rat}}$
$P_{rat}$	rated machine power
$\delta$	rotor current phase angle in degrees
$\Delta$	small perturbation
$T_e$	electric Torque
V	voltage
I	current
$n_p$	pole pairs
P	d/dt
$\omega_m$	rotor angular velocity rad/sec.
$\omega_s$	supply angular velocity rad/sec.
S	slip

#### Suffixes

s	stator
r	rotor
d	d-axis
q	q-axis
	maximum value
	steady state operating point

#### REFERENCES

1. M.A. Saleh, A.M. Issawi, M.N. Iskander, "Double Excited Induction Generators Operating with WECS" ICEM 84 Proceeding, 18-21 Sept. 1984, Part 3, pp. 1064-1067, Lausanne, Switzerland.
2. K. Oguchi, K. Sugawara, Y. Kakizume, "A Stabilized Doubly Fed Motor with a Separately Controlled Current Source Converter" IEEE Trans. Vol. 28, No. 4, pp. 336-341, Nov. 1981.
3. J.C. Prescott, B.P. Raju, "The Inherent Instability of Induction Motor Under Conditions of Double Supply" IEE Monograph, No. 282 U, pp. 319-329, Jan. 1958.

4. B.M. Bird, R.F. Burbidge, "Analysis of Doubly Fed Slip-Ring Machines" Proc. IEE, Vol. 113, No. 6, pp. 1016-1020, June 1966.
5. M. Ohi, J.G. Kassakian, "Dynamic Characteristics and Speed Feedback Stabilization of the Doubly Fed Machine" IEEE PES Summer Meeting, Portland, O.R., pp. 1-8, July 1976.

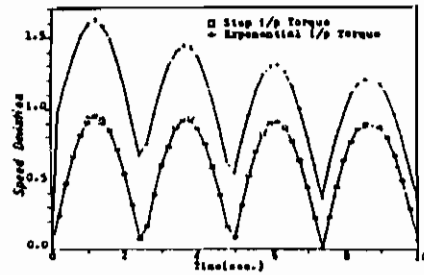


Fig. (11) Speed Deviation for Unstable DFIM

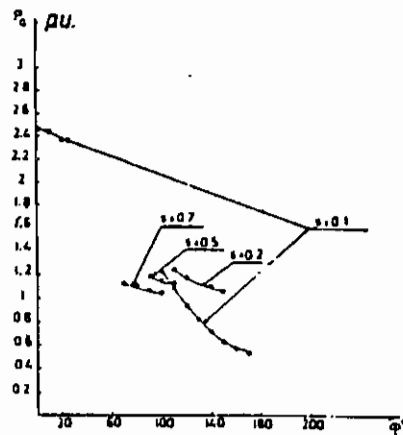


Fig. (12a) Variation of  $P_0$  with  $\phi$  at  $V_1 = 0.05 V_0$  at subsync. speeds

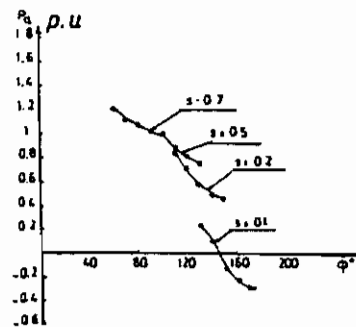
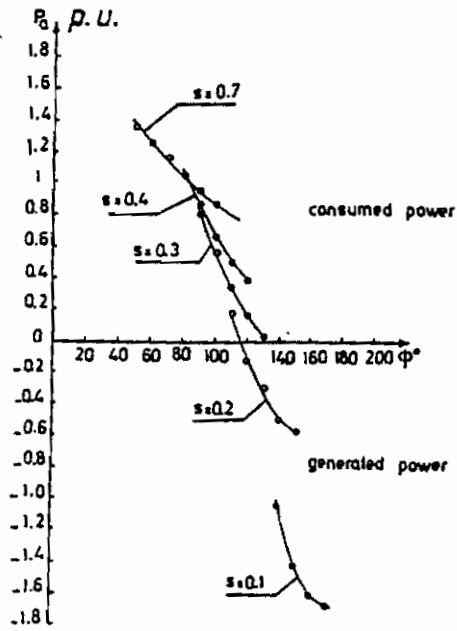
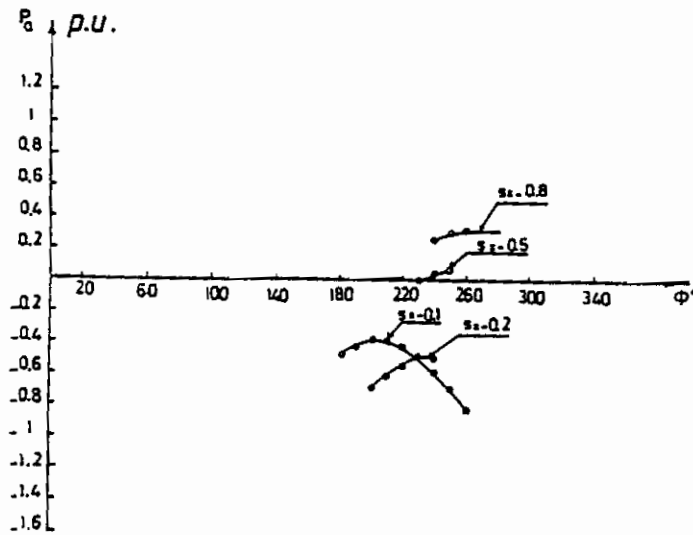


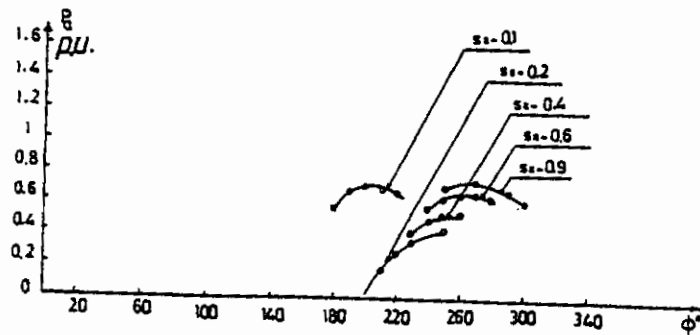
Fig. (12b) Variation of  $P_0$  with  $\phi$  at  $V_1 = 0.1 V_0$  at subsync. speeds.



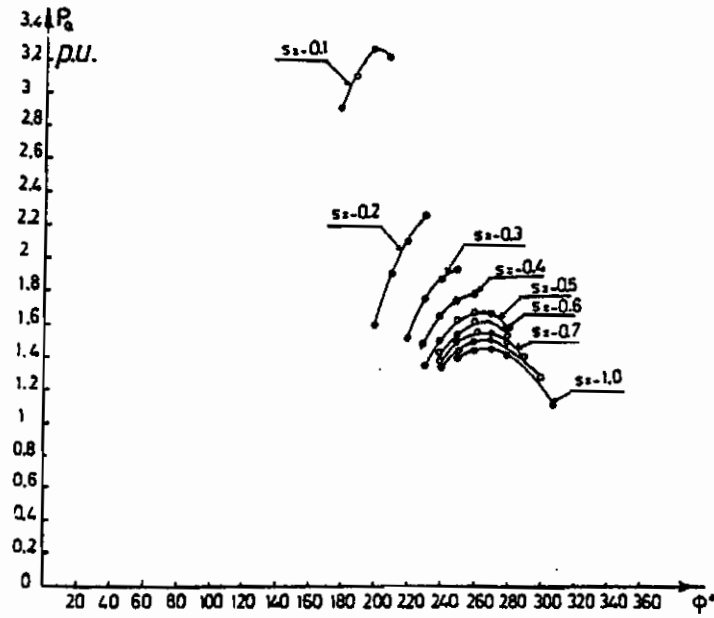
Fig(3) Variation of  $P_0$  with  $\phi$  at  $V_r = 0.2 V_s$  at subsync. Speeds



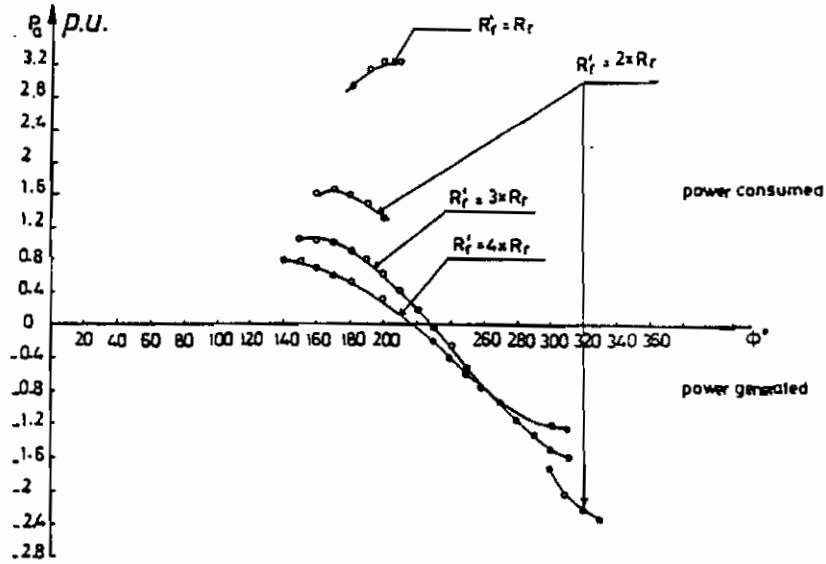
Fig(4) Variation of  $P_0$  with  $\phi$  at  $V_r = 0.05 V_s$  at supersync. Speed



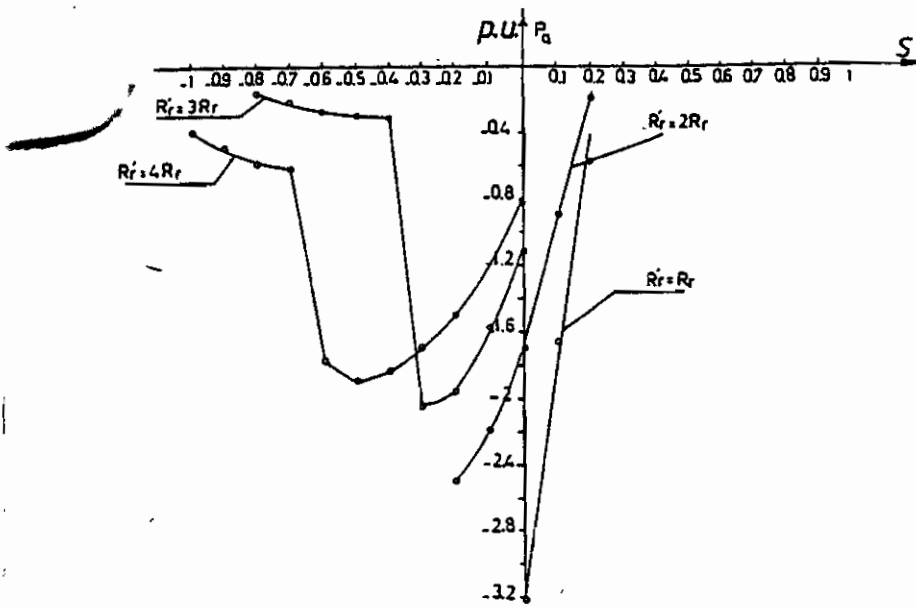
Fig(5) Variation of  $P_0$  with  $\phi$  at  $V_r = 0.1 V_s$  at supersync. Speeds



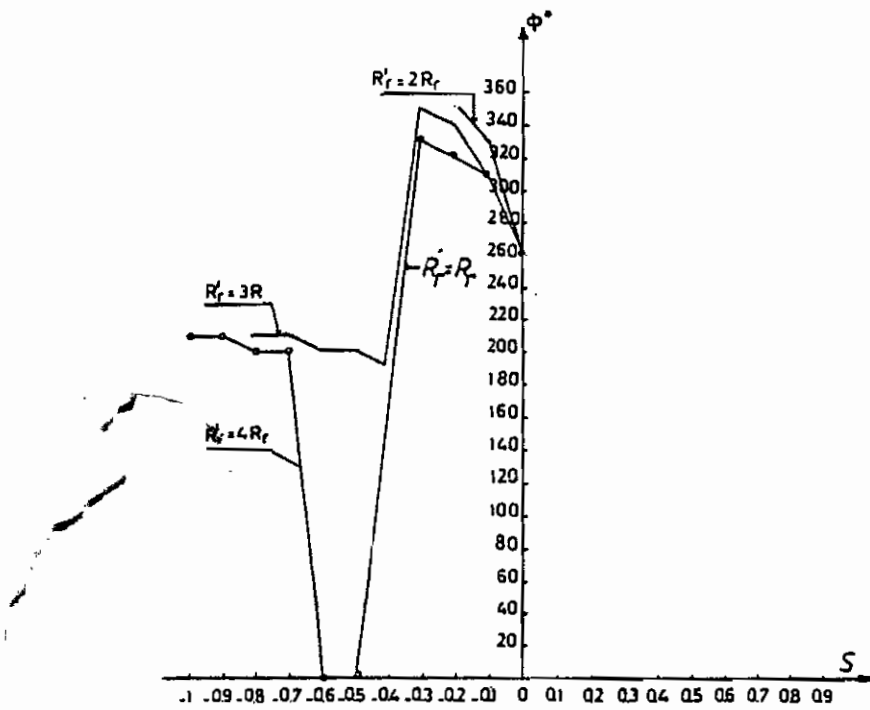
Fig(6) Variation of  $P_g$  with  $\phi$  at  $V_r=0.2V_s$  at supersync. Speeds



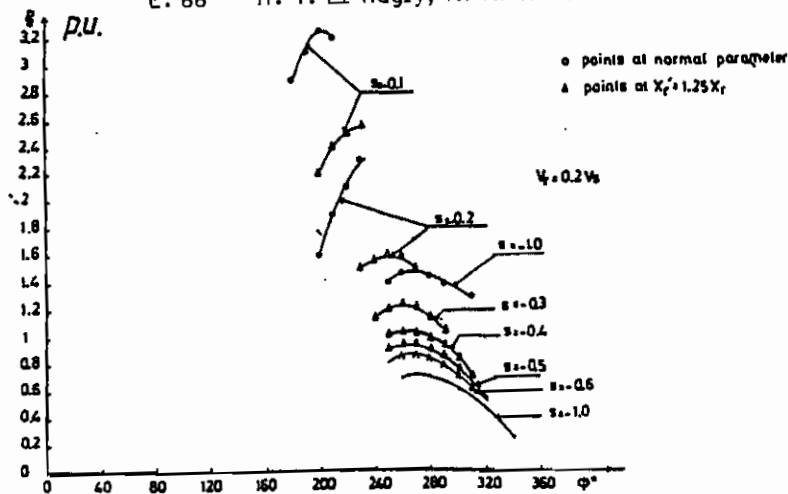
Fig(7) Effect of rotor resistance on power generation at negative slip at  $s=-0.1$ ,  $V_r=0.2V_s$ .



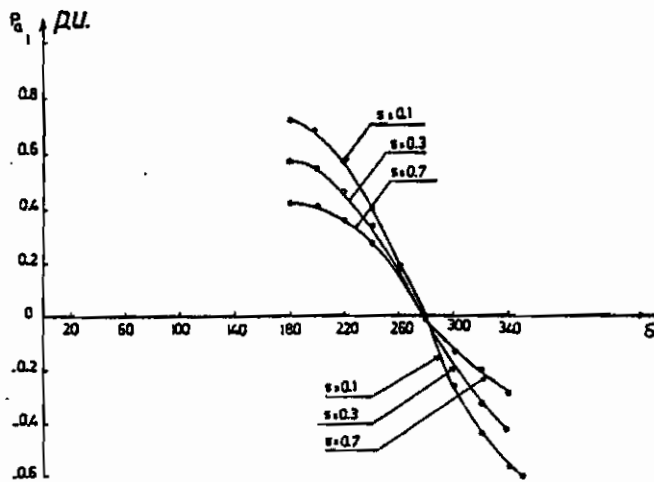
Fig(8) Maximum power generated at different values of rotor resistance.



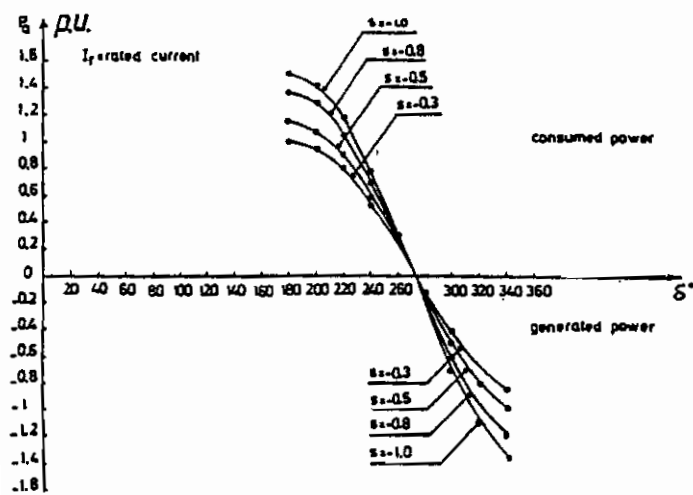
Fig(9) Angles at which maximum power is generated stably as  $R_r$  is Varied.



Fig(10) Effect of increasing rotor reactance on active power of DEIM



Fig(11) Variation of  $P_a$  with  $\delta$  for CSI at subsync. Speeds



Fig(12) Variation of  $P_a$  with  $\delta$  for CSI at supersync. Speeds